

Bufadienolides from *Helleborus foetidus* and their cytotoxic properties on MCF-7 breast cancer cells

Olivier Potterat^{a,*}, Marina Kaufmann^{a,1}, Cécile Tschopp^{a,1}, Michaela Caj^b, Jakob K. Reinhardt^{a,2}, Alessandro Prescimone^c, Devika Shah^{d,e}, Stephan Baumgartner^{e,f}, Michel-Angelo Sciotti^b, Laura Suter-Dick^b

^a Division of Pharmaceutical Biology, University of Basel, Klingelbergstrasse 50, CH-4056, Basel, Switzerland

^b Institute for Chemistry and Bioanalytics, School of Life Sciences, University of Applied Sciences and Arts Northwestern Switzerland, Hofackerstrasse 30, CH-4132, Muttenz, Switzerland

^c University of Basel, Department of Chemistry, Mattenstrasse 22, CH-4058, Basel, Switzerland

^d Iscador AG, Kirschweg 9, CH-4144, Arlesheim, Switzerland

^e Association for Cancer Research, Hiscia Institute, Kirschweg 9, CH-4144, Arlesheim, Switzerland

^f Institute for Integrative Medicine, University of Witten/Herdecke, Gerhard-Kienle-Weg 4, D-58313, Herdecke, Germany

ARTICLE INFO

Keywords:

Helleborus foetidus
Ranunculaceae
Bufadienolides
Cytotoxicity
MCF-7 cells

ABSTRACT

Twelve bufadienolides and six 19-norbufadienolides were isolated from the aerial parts of *Helleborus foetidus*. They consist of aglycons and glucosides and include nine previously undescribed compounds and a compound reported for the first time as a genuine natural product. Their structures were established by extensive spectroscopic analysis and the structure and absolute configuration of two previously unreported 3,4-epoxy derivatives were confirmed by single crystal X-ray diffraction analysis. The compounds were tested for their cytotoxicity on MCF-7 human breast cancer cells. They show differential cytotoxic activity with IC₅₀ values in the range of 2.4 nM - >10 μM. The potency of the activity strongly correlates with the presence of a C-19 aldehyde group. The data complement the scientific basis underpinning the use of *H. foetidus* in anthroposophic medicine for the integrative treatment of cancer.

1. Introduction

Helleborus foetidus L. (Ranunculaceae) commonly known as stinking hellebore is an herbaceous, perennial plant native to Western and Central Europe with extension to Morocco (POWO, 2024; WFO, 2024). The species has also been introduced in Norway and Denmark. While the plant is often considered poisonous, it has been used, besides the more commonly applied species *H. niger* L., in anthroposophic medicine for integrative cancer therapy (Meyer et al., 2024). Characteristic constituents are steroidal saponins (Iguchi et al., 2020a; Watanabe et al., 2003), bufadienolides (Iguchi et al., 2020b; Yokosuka et al., 2018) and anemonin-related constituents (Prieto et al., 2006; Tschesche et al., 1981). An acylated quercetin glycoside and a phenylethanoid glucoside have also been reported (Prieto et al., 2006). In preliminary experiments, we observed that aqueous extracts from the vegetative and

generative parts of *H. foetidus* collected in winter and summer showed strong cytotoxicity against MCF-7 (Michigan Cancer Foundation-7) breast cancer cells (IC₅₀ 3.1–5.5 μg/mL, Supporting Information). HPLC separation of these extracts followed by cytotoxicity testing of the fractions using an approach referred to as HPLC-based activity profiling (Potterat and Hamburger, 2014) revealed the activity to be correlated with the presence of peaks that could be tentatively assigned to bufadienolides in the HPLC-MS trace (Supporting Information). This prompted us to undertake a comprehensive investigation of the bufadienolide constituents of *H. foetidus* which resulted in the isolation of 18 bufadienolide derivatives including nine previously unreported congeners and a compound described for the first time as a genuine natural product. We report here on their isolation, characterization and cytotoxicity assessment.

* Corresponding author. Pharmaceutical Biology, University of Basel, Klingelbergstrasse 50, CH-4056, Basel, Switzerland.

E-mail address: olivier.potterat@unibas.ch (O. Potterat).

¹ These authors contributed equally.

² Present address: Northeastern University, Boston, MA, United States.

2. Results and discussion

Fresh aerial parts from *Helleborus foetidus* were extracted with methanol. The methanol extract was partitioned between water and dichloromethane followed by *n*-butanol. The dichloromethane and *n*-butanol-soluble fractions were fractionated by a combination of chromatographic methods including Sephadex LH-20 column chromatography, medium pressure liquid chromatography (MPLC), and preparative and semi-preparative HPLC. During the separation process, the fractions were analyzed by HPLC-PDA-MS to locate bufadienolides recognizable by their typical UV spectrum with an absorption maximum around 295–300 nm. Targeted isolation afforded **9** from the dichloromethane-soluble fraction and **1–8** and **10–18** from the *n*-butanol-soluble fraction. Compounds **1–7** were identified as 16 β -formyloxy-10 β ,14 β -dihydroxy-5 β -[(β -D-glucopyranosyl)oxy]-19-norbufa-3,20,22-trienolide (**1**) (Iguchi et al., 2020b), scilliglucoside (**2**) (Lichti et al., 1973), 10 β ,14 β ,16 β -trihydroxy-5 β -[(β -D-glucopyranosyl)oxy]-19-norbufa-3,20,22-trienolide (**3**) (Yokosuka et al., 2018), 11 α -hydroxyscilliglucoside (**4**) (Krenn et al., 2000), hellebrigenin-3-O- β -D-glucopyranoside (**5**) (Yang et al., 2010), 3 β ,10 β ,14 β ,16 β -tetrahydroxy-19-norbufa-4,20,22-trienolide (**6**) (Iguchi et al., 2020b), and 3 β ,11 α ,14 β -trihydroxy-19-oxobufa-4,20,22-trienolide (**7**) (Iguchi et al., 2020b) by comprehensive spectroscopic analysis and

comparison with literature data when available (Fig. 1). Their ^1H and ^{13}C NMR data are reported in the Supporting Information. Compounds **1**, **3**, **4**, **6**, and **7** were already reported in *H. foetidus*, (Iguchi et al., 2020b; Yokosuka et al., 2018), while compound **5** was previously described in the genus *Helleborus*, namely in *H. thibetanus* Franch. (Yang et al., 2010) and *H. orientalis* Lam. (Watanabe et al., 2003). Compound **2** was not previously found in the genus *Helleborus*, but was isolated from *Drimys maritima* (L.) Stearn (Syn. *Urginea maritima* (L.) Baker, Asparagaceae) (Lichti et al., 1973).

Compounds **8–18** showed an UV absorption maximum around 295 nm in line with a bufadienolide core structure. Compound **8** had a molecular formula of $\text{C}_{24}\text{H}_{32}\text{O}_7$ which was determined based on the protonated molecular ion at m/z 433.2218 $[\text{M}+\text{H}]^+$ (calcd for $\text{C}_{24}\text{H}_{33}\text{O}_7$ 433.2226) in conjunction with ^{13}C and DEPT NMR data. The ^1H NMR spectrum exhibited characteristic signals for a 2-pyrone ring [δ_{H} 7.54 (d, $J = 2.6$ Hz, H-21), 7.88 (dd, $J = 9.6, 2.6$ Hz, H-22) and 6.29 (dd, $J = 9.6, 0.6$ Hz, H-23)], an angular methyl group [δ_{H} 0.64 (s, H₃-18)], a hydroxymethyl group (δ_{H} 3.64, m and 4.36, t, $J = 4.7$ Hz, OH), and three oxygenated methines [δ_{H} 3.82 (m, H-11), 3.32 (H-3), and 2.83 (d, $J = 3.7$ Hz, H-4)]. The ^{13}C NMR spectrum revealed the presence of 24 carbon signals consisting of one methyl group, eight methylenes, nine methines, and six non-protonated carbons, the latter including two oxygenated sp^3 carbons. These data together with the molecular formula fit with a

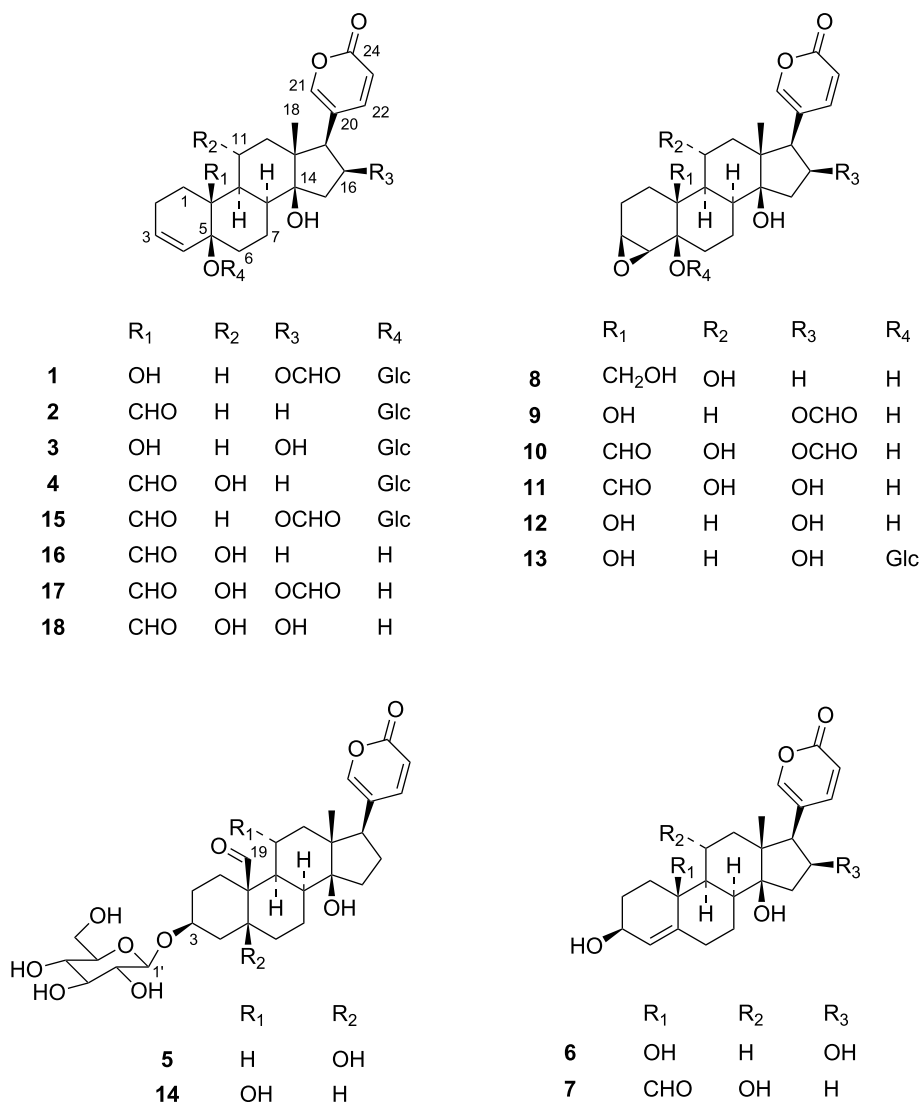


Fig. 1. Structures of compounds **1–18**.

bufadienolide containing an epoxy ring and four hydroxyl groups. Two tertiary OH groups were located at C-5 (δ_C 69.8), and C-14 (δ_C 83.2) based on the downfield resonance of these carbons and HMBC correlations of the hydroxyl groups to neighboring carbons (Fig. 2). A secondary hydroxyl group at C-11 (δ_H 4.15, d, $J = 5.2$ Hz) was revealed by the COSY correlation of the hydroxyl proton to H-11 (δ_H 3.82) and the correlations of H-11 to H₂-12 (δ_H 1.53 and 1.39). Its alpha orientation was revealed by the ROESY correlation between H-11 and CH₃-18 (δ_H 0.64). The hydroxymethyl group was located at C-10 based on the HMBC correlations of OH-19 to C-10 (δ_C 41.9) and C-19 (δ_C 62.9). The position of the epoxy group at C-3/C-4 was revealed by the HMBC correlations from H-4 (δ_H 2.83) to C-5 (δ_C 69.8), C-6 (δ_C 36.4), and C-10 (δ_C 41.9). The orientation of the epoxy group was inferred from the ROESY correlations observed between H α -7 (δ_H 0.98) and H-4, and H α -6 (δ_H 1.58) and H-4. The orientation of the epoxy group and the full structure, including the absolute configuration, were eventually confirmed by X-ray analysis of a crystal grown in ethanol-*n*-hexane (Fig. 3). ¹H and ¹³C NMR data of **8** are shown in Tables 1 and 2. This is the first reported description of the structure 5 β ,11 α ,14 β ,19-tetrahydroxy-3 β ,4 β -epoxybufa-20,22-dienolide, named hellefoetin A.

Compound **9** had a molecular formula of C₂₄H₃₀O₈ which was determined based on the protonated molecular ion at m/z 447.2009 [M+H]⁺ (calcd for C₂₄H₃₁O₈ 447.2018) together with ¹³C and DEPT NMR data. The ¹H NMR spectrum exhibited the characteristic signals of a 2-pyrone ring, and an angular methyl group as in **8**. In addition, the presence of three oxygenated methines [δ_H 5.46 (dd, $J = 8.9$, 8.9 Hz, H-16), 3.24 (m, H-3), 2.97 (d, $J = 3.4$ Hz, H-4)] and a formyloxy group [δ_H 8.00 (s, H-25)] was revealed. The ¹³C NMR spectrum revealed the presence of 24 carbon signals consisting of one methyl group, seven methylenes, ten methines and six non-protonated carbons, the latter including three oxygenated sp³ carbons. These data together with the molecular formula were consistent with a bufadienolide containing an epoxy, three hydroxyl groups (δ_H 3.41, 3.97, 4.50, 3 s) and a formyloxy substituent (δ_H 8.00, s). The three OH groups were located at C-5 (δ_C

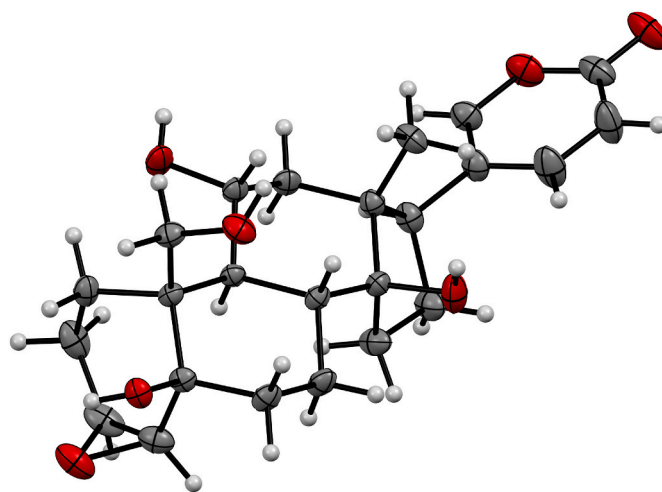


Fig. 3. ORTEP Diagram of compound **8**.

68.7), C-10 (δ_C 71.6) and C-14 (δ_C 82.1) based on the downfield resonance of these carbons and HMBC correlations of the hydroxyl groups to neighboring carbons (Fig. 2). The position of the formyloxy group was indicated by the HMBC correlation of the formyl proton at δ_H 8.00 (H-25) to δ_C 73.6 (C-16). Its β -orientation was deduced from the coupling constant ($J = 8.9$ Hz) between H-16 (δ_H 5.46) and H-17 (δ_H 2.92) as well as the ROESY correlation observed between these protons. The position of the epoxy group at C-3/C-4 was revealed by the HMBC correlations between H-3 (δ_H 3.24) and C-2 (δ_C 22.2) as well as from H-4 (δ_H 2.97) and C-5 (δ_C 68.7) and C-10 (δ_C 71.6). Its orientation was inferred from the ROESY correlation between H α -7 (δ_H 0.86) and H-4 and the strong similarity of the ¹H and ¹³C NMR chemical shifts with those of **8**. The ¹H and ¹³C NMR data of **9** are shown in Tables 1 and 2. This is the first report of the structure 16 β -formyloxy-5 β ,10 β ,14 β -trihydroxy-3 β ,4 β -

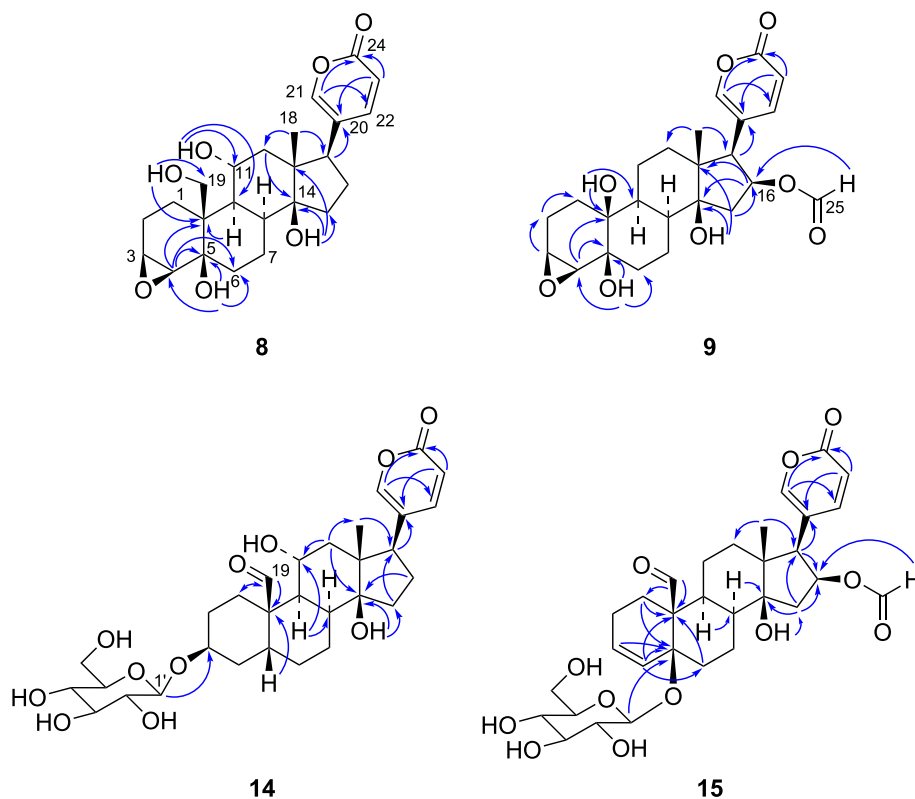


Fig. 2. Key HMBC correlations of compounds **8**, **9**, **14**, and **15**.

Table 1¹³C NMR data of compounds 8–18 (DMSO-*d*₆, 126 MHz).

Position	8	9	10	11	12	13	14	15	16	17	18
1	19.2, CH ₂	22.5, CH ₂	17.5, CH ₂	17.2, CH ₂	22.2, CH ₂	22.3, CH ₂	32.8, CH ₂	19.1, CH ₂	23.8, CH ₂	22.2, CH ₂	21.8, CH ₂
2	21.2, CH ₂	22.2, CH ₂	20.5, CH ₂	20.4, CH ₂	22.6, CH ₂	22.8, CH ₂	30.7, CH ₂	20.9, CH ₂	28.2, CH ₂	21.9, CH ₂	21.9, CH ₂
3	53.9, CH	53.7, CH	53.0, CH	53.0, CH	53.6, CH	51.9, CH	75.5, CH	131.6, CH	130.0, CH	130.1, CH	129.9, CH
4	58.7, CH	57.8, CH	57.8, CH	57.8, CH	57.9, CH	57.6, CH	35.7, CH ₂	129.6, CH	133.5, CH	133.4, CH	133.5, CH
5	69.8, C	68.7, C	69.6, C	69.6, C	68.8, C	74.9, C	53.4, CH	76.6, C	70.6, C	70.6, C	70.6, C
6	36.4, CH ₂	34.8, CH ₂	36.7, CH ₂	36.7, CH ₂	34.9, CH ₂	29.5, CH ₂	28.8, CH ₂	33.3, CH ₂	37.0, CH ₂	36.8, CH ₂	36.8, CH ₂
7	23.0, CH ₂	22.7, CH ₂	22.8, CH ₂	23.0, CH ₂	22.9, CH ₂	23.0, CH ₂	27.4, CH ₂	23.4, CH ₂	21.9, CH ₂	23.4, CH ₂	23.6, CH ₂
8	40.1, CH	39.0, CH	40.8, CH	40.7, CH	39.2, CH	39.4, CH	41.8, CH	41.4, CH	40.7, CH	40.9, CH	40.9, CH
9	43.4, CH	39.2, CH	43.0, CH	43.3, CH	39.3, CH	39.4, CH	42.8, CH	38.1, CH	43.9, CH	43.5, CH	43.7, CH
10	41.9, C	71.6, C	52.3, C	52.4, C	71.6, C	72.4, C	52.1, C	52.3, C	53.1, C	52.9, C	53.0, C
11	67.5, CH	19.7, CH ₂	66.7, CH	66.7, CH	19.8, CH ₂	19.6, CH ₂	66.7, CH	22.2, CH ₂	67.0, CH	66.6, CH	66.7, CH
12	50.6, CH ₂	38.9, CH ₂	49.3, CH ₂	49.0, CH ₂	39.6, CH ₂	39.6, CH ₂	50.2, CH ₂	38.8, CH ₂	50.2, CH ₂	49.4, CH ₂	49.2, CH ₂
13	48.5, C	48.8, C	49.3, CH ₂	48.7, C	48.5, C	48.5, C	48.2, C	48.8, C	48.4, C	49.3, C	48.7, C
14	83.2, C	82.1, C	81.7, C	82.3, C	82.8, C	82.6, C	82.5, C	82.1, C	82.7, C	81.7, C	82.4, C
15	31.6, CH ₂	40.0, CH ₂	39.8, CH ₂	41.9, CH ₂	42.5, CH ₂	42.4, CH ₂	31.8, CH ₂	39.2, CH ₂	31.3, CH ₂	39.2, CH ₂	41.9, CH ₂
16	28.4, CH ₂	73.6, CH	73.7, CH	70.9, CH	70.5, CH	70.5, CH	28.2, CH ₂	73.5, CH	22.1, CH ₂	73.7, CH	70.8, CH
17	49.8, CH	55.5, CH	54.9, CH	56.1, CH	57.4, CH	57.4, CH	49.7, CH	55.4, CH	49.6, CH	54.9, CH	56.1, CH
18	18.0, CH ₃	16.4, CH ₃	17.7, CH ₃	18.6, CH ₃	16.6, CH ₃	16.6, CH ₃	17.5, CH ₃	16.4, CH ₃	17.8, CH ₃	17.8, CH ₃	18.6, CH ₃
19	62.9, CH ₂	–	207.5, CH	207.4, CH	–	–	209.6, CH	207.3, CH	208.4, CH	208.4, CH	208.4, CH
20	122.4, C	117.1, C	116.6, C	118.2, C	118.7, C	118.7, C	122.2, C	117.0, C	122.2, C	116.7, C	118.2, C
21	149.3, CH	151.4, CH	151.6, CH	150.5, CH	150.3, CH	150.3, CH	149.5, CH	151.5, CH	149.4, CH	151.6, CH	150.4, CH
22	147.3, CH	150.1, CH	149.8, CH	150.9, CH	151.5, CH	151.5, CH	147.2, CH	150.0, CH	147.2, CH	149.7, CH	150.9, CH
23	114.2, CH	111.9, CH	112.1, CH	111.4, CH	111.0, CH	111.0, CH	114.3, CH	111.9, CH	114.3, CH	112.0, CH	111.4, CH
24	161.4, C	161.4, C	161.1, C	161.6, C	161.7, C	161.7, C	161.3, C	161.1, C	161.3, C	161.4, C	161.6, C
25	–	161.2, CH	161.4, CH	–	–	–	–	161.4, CH	–	161.1, CH	–
1'	–	–	–	–	–	96.6, CH	100.5, CH	96.9, CH	–	–	–
2'	–	–	–	–	–	73.9, CH	73.5, CH	73.6, CH	–	–	–
3'	–	–	–	–	–	76.8, CH	76.7, CH	77.0, CH	–	–	–
4'	–	–	–	–	–	70.4, CH	70.1, CH	70.2, CH	–	–	–
5'	–	–	–	–	–	76.8, CH	76.8, CH	76.4, CH	–	–	–
6'	–	–	–	–	–	61.3, CH ₂	61.1, CH ₂	61.2, CH ₂	–	–	–

Table 2¹H NMR data of compounds 8–12 (DMSO-*d*₆, 500 MHz)^a.

Position	8	9	10	11	12					
1 α	1.70	1.88	2.29	br dd (13.3, 3.8)	2.19	br dd (13.1, 4.0)	1.47			
1 β	1.23	1.80	1.66		1.64	ddd (13.1, 13.0, 4.7)	1.12	dd (13.4, 5.2)		
2 α	2.12	1.48	2.15		2.13		1.76			
2 β	1.72	m	1.12	br dd (13.6, 5.0)	1.85		1.87			
3	3.32	3.24	m		3.35		3.24	m		
4	2.83	d (3.7)	2.97	d (3.7)	2.90	d (3.7)	2.97	d (3.4)		
6 α	1.58	1.61	1.84		1.84		1.60	m		
6 β	2.04	1.75	1.94		1.95	ddd (13.6, 12.2, 3.1)	1.76			
7 α	0.98	m	0.86	m	1.00	ddd (14.4, 12.2, 11.6)	0.88	m		
7 β	1.96	1.93	2.11		2.12		1.93			
8	1.89	1.57	m	1.89	1.83		1.52			
9	1.37	1.27	1.43	br dd (11.1, 11.1)	1.39	dd (11.6, 10.1)	1.22			
11/11 α	3.82	m	1.29	m	3.42	m	1.27			
11 β		1.39					1.36			
12 α	1.39	1.38	1.34	dd (13.3, 10.7)	1.30	br dd (13.1, 10.4)	1.30			
12 β	1.53	1.43	1.54	dd (13.3, 4.0)	1.46	br dd (13.1, 4.0)	1.41			
15 α	1.94	2.54	dd (15.3, 8.9)	2.56	dd (15.6, 8.5)	2.35	dd (14.3, 7.6)	2.34	dd (14.6, 8.2)	
15 β	1.54	1.64	1.68		1.56	br d (14.3)	1.53			
16/16 α	2.04	5.46	dd (8.9, 8.9)	5.47	dd (8.9, 8.5)	4.42	m	4.41	m	
16 β	1.61									
17	2.50	2.92	d (8.9)	2.96	d (8.9)	2.74	br d (7.6)	2.64	d (8.2)	
18	0.64	s	0.67	s	0.69	s	0.66	s	0.64	s
19	3.64	m		9.77	s		9.78	s		
21	7.54	br d (2.6)	7.55	d (1.8)	7.56	d (2.4)	7.52	d (2.1)	7.48	d (2.4)
22	7.88	dd (9.6, 2.6)	8.17	br dd (10.1, 1.8)	8.08	dd (9.8, 2.4)	8.04	dd (9.8, 2.1)	8.10	dd (9.8, 2.4)
23	6.29	dd (9.6, 0.6)	6.20	dd (9.8, 0.6)	6.21	dd (9.8, 0.6)	6.14	d (9.8)	6.12	dd (9.8, 0.9)
25	–	8.00	s	8.01	s	–	–	–	–	–
OH-5	4.05	3.97	s	4.56	s	4.54	s	3.95	3.97	s
OH-10	–	3.41	s	–	–	–	–	3.37	–	s
OH-11	4.15	d (5.2)	–	4.39	d (5.2)	4.37	br d (4.9)	–	–	–
OH-14	4.19	s	4.50	s	4.65	s	4.33	s	4.23	s
OH-16	–	–	–	–	–	4.66	br d (4.3)	4.51	–	d (5.2)
OH-19	4.36	t (4.7)	–	–	–	–	–	–	–	–

^a Overlapped signals are reported without multiplicity; n.a.: not assigned.

epoxy-19-norbufa-20,22-dienolide, named hellefoetin B.

The molecular formula of **10** was found to be $C_{25}H_{30}O_9$ based on HRESIMS data (m/z 475.1950 $[M+H]^+$, calcd for $C_{25}H_{31}O_9$ 475.1968) in conjunction with ^{13}C NMR data. The 1H NMR spectrum revealed a bufadienolide skeleton with an epoxide ring [δ_H 3.35 (s, H-3) and 2.90 (d, $J = 3.7$ Hz, H-4)], a formyloxy group [δ_H 8.01 (s, H-25)], an aldehyde proton [δ_H 9.77 (s, H-19)], one secondary (δ_H 4.39, d, $J = 5.2$ Hz) and two tertiary (δ_H 4.65, 4.56, 2 s) OH groups. The position and orientation of the formyloxy substituent and the two tertiary OH groups were identical as in **9** as revealed by COSY, HMBC, and ROESY correlations. The aldehyde group was assigned to C-19 based on the HMBC correlations of H-19 (δ_H 9.77) to C-1 (δ_C 17.5) and C-10 (δ_C 52.3). The location of the secondary hydroxyl group (δ_H 4.39, d, $J = 5.2$ Hz) was inferred from the COSY correlation of the hydroxyl proton to H-11 (δ_H 3.45) and the correlations of H-11 to H₂-12 (δ_H 1.54 and 1.34). Its alpha orientation was revealed by the ROESY correlation between H-11 and CH₃-18 (δ_H 0.69). The 1H and ^{13}C NMR data of **10** are shown in Tables 1 and 2. This is the first description of the structure 16 β -formyloxy-5 β ,11 α ,14 β -trihydroxy-3 β ,4 β -epoxy-19-oxobufa-20,22-dienolide, named hellefoetin C.

The molecular formula of **11** was established as $C_{24}H_{30}O_8$ from the HRESIMS data (m/z 447.2009 $[M+H]^+$, calcd for $C_{24}H_{31}O_8$ 447.2018) and ^{13}C NMR data. Compound **11** had similar 1D and 2D (COSY, HMBC, and HSQC) NMR data to those of **10**. The differences were due to the presence of a hydroxyl group instead of a formyloxy group at C-16. Accordingly, C-16 was upfield shifted to δ_C 70.9 compared to δ_C 73.7 in **10**. The beta orientation of OH-16 was revealed by the coupling constant between H-16 (δ_H 4.42) and H-17 (δ_H 2.74, d, $J = 7.6$ Hz) and was further supported by the ROESY correlation between H-16 and H-17. The full structure including the absolute configuration was finally confirmed by single crystal X-ray diffraction analysis (Fig. 4). The 1H and ^{13}C NMR data of **11** are listed in Tables 1 and 2. This is the first report of the structure 5 β ,11 α ,14 β ,16 β -tetrahydroxy-3 β ,4 β -epoxy-19-oxobufa-20,22-dienolide, named hellefoetin D.

Compound **12** had the molecular formula $C_{23}H_{30}O_7$ as revealed by the protonated molecular ion in HRESIMS (m/z 419.2053 $[M+H]^+$, calcd for $C_{23}H_{31}O_7$ 419.2069) and ^{13}C NMR data. The compound had similar 1D (1H , ^{13}C) and 2D (COSY, HMBC, and HSQC) NMR data to those of **11**. The differences were due to the presence of a hydroxyl group at C-10 (δ_C 71.6) instead of a formyl group and the lack of the hydroxyl group at C-11. The 1H and ^{13}C NMR data of **12** are shown in Tables 1 and 2. The compound, named here hellefoetin E, has been very recently described in a Chinese patent application (Yang et al., 2024). However, no evidence was provided for the reported configuration.

Compound **13** had a molecular weight of 580 amu from the quasi-molecular ions at m/z 579 $[M-H]^-$ and at m/z 581 $[M+H]^+$ in the ESIMS spectra. A prominent fragment ion peak at m/z 419 ($[(M+H)-162]^+$) suggested compound **13** to be a hexoside. Acid hydrolysis

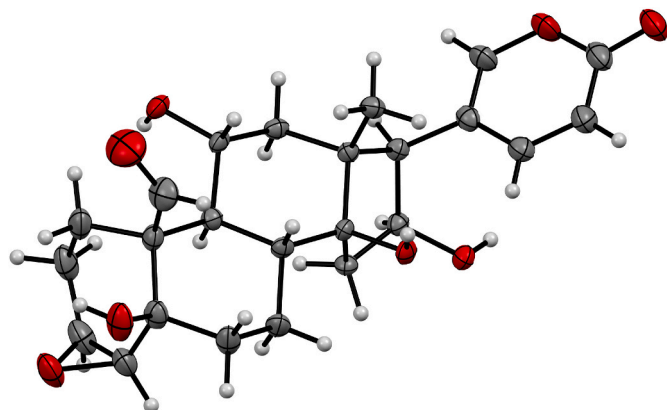


Fig. 4. ORTEP diagram of compound **11**.

yielded D-glucose which was identified by GC analysis after derivatization with (+)-2-butanol acetyl chloride. The molecular formula $C_{29}H_{40}O_{12}$ was elucidated based on HRESIMS data (m/z 581.2591 $[M+H]^+$, calcd for $C_{29}H_{41}O_{12}$ 581.2598) in conjunction with ^{13}C NMR data. The 1H and ^{13}C NMR data were highly similar to those of **11**, but characteristic signals were observed for a β -glucopyranosyl group [δ_H 4.55 (d $J = 7.6$ Hz, H-1'), δ_C 96.6 (C-1'), 73.9 (C-2'), 76.8 (C-3'), 70.4 (C-4'), 76.8 (C-5') and 61.3 (C-6')] in the ^{13}C NMR spectrum. The linkage of the β -D-glucopyranosyloxy group to C-5 was revealed by the HMBC cross peak between δ_H 4.48 (H-1') and δ_C 74.9 (C-5). Compound **13** is therefore 10 β ,14 β ,16 β -trihydroxy-5 β -[(β -D-glucopyranosyl)oxy]-3 β ,4 β -epoxy-19-norbufa-20,22-dienolide, the 5-O-glucoside of **11**. The 1H and ^{13}C NMR data of **13** are shown in Tables 1 and 3. The planar structure of **13**, named hellefoetinoside A, was already mentioned in a patent application but no spectroscopic data have been reported (Djaballah et al., 2013).

The molecular formula of **14** was established as $C_{30}H_{42}O_{11}$ based on HRESIMS data (m/z 579.2814 $[M+H]^+$, calcd for $C_{30}H_{43}O_{11}$ 579.2805) in conjunction with ^{13}C NMR data. Acid hydrolysis afforded D-glucose. The NMR data showed the signals corresponding to a beta-glucopyranosyl residue, a formyl group (δ_H 9.94, s; δ_C 209.6) and two hydroxyl groups (δ_H 4.28, 4.44) in agreement with the molecular formula. NMR data of **14** were similar to those of **5**. The difference was due to the presence of a hydroxyl group at C-11 instead of C-5. The linkage of the hydroxyl group at C-11 was indicated by the HMBC cross peaks between δ_H 1.53 (H-12) and δ_H 1.26 (H-9) to δ_C 66.7 (C-11) (Fig. 2). The location of the glucopyranosyloxy moiety at C-3 was supported by the HMBC correlation between H-1' (δ_H 4.20, d, $J = 7.9$ Hz) and C-3 (δ_C 75.5). 1H and ^{13}C NMR data of **14** are shown in Tables 1 and 3. This is the first report of the structure 11 α ,14 β -dihydroxy-3 β -[(β -D-glucopyranosyl)oxy]-19-oxobufa-20,22-dienolide, named hellefoetinoside B.

The molecular formula of **15** was deduced to be $C_{31}H_{40}O_{12}$ from the protonated molecular ion at m/z 605.2602 $[M+H]^+$ in the HRESIMS spectrum (calcd for $C_{31}H_{41}O_{12}$ 605.2598) together with ^{13}C and DEPT NMR data. Acid hydrolysis followed by GC-analysis revealed the presence of D-glucose. The NMR data (Tables 1 and 3) showed the presence of an olefinic bond (δ_C 131.6, d; 129.6, d) in addition to the unsaturated δ lactone ring, formyl and formyloxy groups, and a beta glucopyranosyl residue. The beta glucopyranosyloxy moiety was located at C-5 like in **13** from the HMBC correlation from H-1' (δ_H 4.35 d, $J = 7.9$) to C-5 (δ_C 76.6) (Fig. 2). The formyloxy was at C-16 (δ_C 73.5) in beta-orientation and the aldehyde was at C-19 (δ_H 9.94, δ_C 207.3) like in the other isolated bufadienolides possessing these functional groups. The olefinic bond was located at C-3,4 from the HMBC correlation between H-3 (δ_H 5.90, m) and C-5 and between H-4 (δ_H 5.48, br d, $J = 10.1$) and C-5, C-6 (δ_C 33.1), and C-10 (δ_C 52.3). The structure was therefore elucidated as 16 β -formyloxy-14 β -hydroxy-5 β -[(β -D-glucopyranosyl)oxy]-19-oxobufa-3,20,22-trienolide, a previously undescribed bufadienolide, named hellefoetinoside C.

Compound **16** had a molecular formula of $C_{24}H_{30}O_6$ based on HRESIMS data (m/z 415.2104 $[M+H]^+$, calcd for $C_{24}H_{31}O_6$ 415.2120) and ^{13}C NMR data. NMR data revealed the presence of a double bond at C-3 (4) and a formyl group (C-19) like in **15**. In addition to the hydroxyl groups at C-5 (δ_C 70.6) and C-14 (δ_C 82.7), the presence of a hydroxyl group at C-11 (δ_C 67.0) like in **8**, **10**, **11**, and **14** was confirmed by the COSY correlations of H-11 (δ_H 3.43) to H-9 (δ_H 1.34) and H₂-12 (δ_H 1.49, 1.29). Its alpha orientation was supported by the ROESY correlation observed between H-11 and CH₃-18 (δ_H 0.60). 1H and ^{13}C NMR data of **16** are reported in Tables 1 and 3. The compound that was named hellefoetin F was previously obtained as a hydrolysis product of desacetylscillicyanoside, but no spectroscopic data were reported (Yokosuka et al., 2018). Compound **16** is described for the first time as a genuine natural product.

A molecular formula $C_{25}H_{30}O_8$ was established for **17** based on HRESIMS data (m/z 459.2009 $[M+H]^+$, calcd for $C_{25}H_{31}O_8$ 459.2018) in conjunction with ^{13}C NMR data. The NMR data were similar to those

Table 3

¹H NMR data of compounds 13–18 (DMSO-*d*₆, 500 MHz)^a.

Position	13	14	15	16	17	18
1 α	1.70	1.11	1.97	2.59	2.60	2.51
1 β	1.05	3.14	1.73	1.94	1.97	1.96
2 α	1.76	1.82	2.03	2.15	2.17	2.15
2 β	1.84	1.12	1.94	1.94	1.93	1.95
3	3.09	3.59	5.90	5.82	5.84	5.83
4/4 α	2.91	1.82	5.48	5.34	5.34	5.35
4 β		1.20				
5		1.23				
6 α	1.90	1.45	2.00	1.63	1.62	1.62
6 β		1.80	2.09	1.85	1.83	1.84
7 α	0.91	1.05	0.88	0.93	0.87	0.90
7 β	2.04	2.14	2.11	2.01	2.02	2.02
8	1.50	1.42	1.70	1.85	1.88	1.79
9	1.27	1.26	1.32	1.34	1.30	1.27
11/11 α	1.26	3.57	1.35	3.43	3.46	3.44
11 β	1.41		0.94			
12 α	1.32	1.31	1.31	1.29	1.29	1.25
12 β	1.39	1.53	1.38	1.49	1.54	1.48
15 α	2.35	1.89	2.41	1.81	2.39	2.21
15 β	1.54	1.56	1.61	1.48	1.65	1.50
16/16 α	4.42	2.05	5.43	2.03	5.43	4.38
16 β		1.58		1.59		
17	2.64	2.47	2.89	2.47	2.93	2.71
18	0.65	0.55	0.62	0.60	0.69	0.66
19		9.94	9.94	9.89	9.86	9.87
21	7.48	7.54	7.53	7.53	7.55	7.51
22	8.12	7.86	8.13	7.86	8.07	8.03
23	6.13	6.28	6.20	6.29	6.20	6.14
25			7.98		7.99	
1'	4.55	4.20	4.35	–	–	–
2'	3.06	2.86	2.78	–	–	–
3'	3.13	3.11	3.08	–	–	–
4'	3.00	3.00	2.99	–	–	–
5'	3.07	3.06	2.99	–	–	–
6'	3.65	3.64	3.58	–	–	–
	3.38	3.39	3.38	–	–	–
OH-5	–	–	–	n.a.	4.85	4.83
OH-10	3.88	–	–	–	–	–
OH-11	–	4.44	–	n.a.	4.33	4.30
OH-14	4.26	4.28	4.65	n.a.	4.58	4.26
OH-16	4.52	–	–	–	–	4.62
OH-2'	5.51	4.86	4.71	–	–	–
OH-3'	4.97	4.89	n.a.	–	–	–
OH-4'	4.91	4.88	4.84	–	–	–
OH-6'	4.29	4.44	4.13	–	–	–

^a Overlapped signals are reported without multiplicity; n.a.: not assigned.

of **16**, except for the presence in **17** of a formyloxy group which accounted for a difference of 44 amu in their molecular masses. The position of the formyloxy group was indicated by the HMBC correlation of $\delta_{\text{H}} 7.99$ (H-25) to $\delta_{\text{C}} 73.7$ (C-16). Its beta orientation was supported by the coupling constant between H-16 ($\delta_{\text{H}} 5.43$, dd, $J = 8.5, 8.5$) and H-17 ($\delta_{\text{H}} 2.93$, d, $J = 8.5$) as well as the ROESY correlation between these protons. ¹H and ¹³C NMR data of **17** are listed in Tables 1 and 3. This is the first report of the structure 16β-formyloxy-5β,11α,14β-trihydroxy-19-oxobufa-3,20,22-trienolide, named hellefoetin G.

Compound **18** had the molecular formula C₂₄H₃₀O₇ as revealed by the protonated molecular ion in HRESIMS at m/z 431.2074 [$M+H$]⁺ (calcd for C₂₄H₃₁O₇ 431.2069) in conjunction with ¹³C NMR data. The NMR data of **18** were similar to those of **17**, but the formyloxy group at C-16 ($\delta_{\text{C}} 70.8$) in **17** was replaced by a hydroxyl group in **18** which was in agreement with a 2.9 ppm upfield shift of C-16 compared to **17**. The position of the hydroxyl group was confirmed by the HMBC cross peak between $\delta_{\text{H}} 2.71$ (H-17) to $\delta_{\text{C}} 70.8$ (C-16). The ¹H and ¹³C NMR data of **18** are shown in Tables 1 and 3. This is the first description of the

structure 5β,11α,14β,16β-tetrahydroxy-19-oxobufa-20,22-dienolide, named hellefoetin H.

Our targeted investigation of the bufadienolides in *H. foetidus* yielded 18 compounds including nine previously undescribed compounds (**8–11**, **13–15**, **17**, and **18**) and a new natural product (**16**). The structural diversity arises from different substitution combinations at only a limited number of positions, namely C-3, C-4, C-5, and C-10 on ring A, C-11, and C-16. The configuration at these positions is moreover identical in all substituted compounds. Interestingly, there is only a partial overlap between the compounds isolated in this study and bufadienolides described in previous investigations of *H. foetidus*. Only five compounds (**1**, **3**, **4**, **6**, and **7**) out of 18 had been previously reported from this plant, while five compounds previously isolated were not obtained in our study (Iguchi et al., 2020b; Yokosuka et al., 2018). Furthermore, 3,4-epoxybufadienolides, such as compounds **8–13**, are uncommon in nature and were not previously described in *H. foetidus*. The few previous examples include hellebortins B and C from *Helleborus torquatus* Archer-Hind (Meng et al., 2001), compound **12** very recently reported

from *H. thibetanus* (Yang et al., 2024), as well as abyssinin and abyssinols A-C from *Bersama abyssinica* Fresen. (Kubo and Matsumoto, 1984, 1985). The orientation of the epoxide in the former ones could not be determined, while the configuration in abyssinin was established as alpha by NMR analysis after addition Eu (fod)₃. The observed ROESY correlations together with the X-Ray crystallographic data for **8** and **11** will provide useful reference data for the determination of the configuration of 3,4-epoxy bufadienolides in future.

The cytotoxicity of compounds **1–18** and of cisplatin was tested on MCF-7 breast cancer cells. The cell line was selected as one of the most studied human breast cancer cell lines and cisplatin as a comparator, due to its widespread clinical use. The IC₅₀ values are presented in Table 4 and the corresponding concentration-response curves are available in the Supporting Information. The data show strong differences in the potency of the compounds. In this experimental setup, cisplatin led to the expected cytotoxicity, but with a higher than anticipated IC₅₀ (31.5 μM). Under the same experimental conditions, many of the tested compounds showed IC₅₀s in the low nM range. Specifically, compounds **5** and **16** were the most potent with IC₅₀ values of 5.5 nM and 1.4 nM, respectively, while the IC₅₀ of **13** (the least active compound) was >10 μM. Interestingly, all compounds with an IC₅₀ < 100 nM possessed an aldehyde group at C-19, while compounds with IC₅₀ > 600 nM were all devoid of this structural feature. Two compounds with an aldehyde at C-19 (**11** and **14**) and one compound without this group (**8**) showed moderate activity (IC₅₀s 160–533 nM). These results are in line with a previous report which concluded that the aldehyde function is essential for potent cytotoxic activity on HL-60 and A549 cells (Yokosuka et al., 2018). Nevertheless, in a subsequent investigation by the same authors, compound **1**, which is devoid of an aldehyde group and was only weakly active (IC₅₀ 1,020 nM) on MCF-7 cells in our study, was surprisingly found to be among the most potent compounds against HL-60 and A549 cancer cell lines (Iguchi et al., 2020b). Whether these seemingly contradictory results are due to the different cell lines or the presence of strongly active impurities will require further investigation.

There are some conflicting data in literature regarding the bufadienolide content and the role of this group of compounds in the cytotoxic activity observed for *H. foetidus* extracts. Bufadienolides have been described as cytotoxic constituents of *H. foetidus* by Yokosuka and co-workers (Iguchi et al., 2020b; Yokosuka et al., 2018). In a recent study, however, no bufadienolides were detected in water extracts of *H. niger* and *H. foetidus* and the observed cytotoxicity was put in relation with the protoanemonin and saponin contents (Müller et al., 2023). Different

extracts, harvesting times or biological variation have been put forward by the authors to explain these seemingly contradictory findings. In this context it is worth noting that we detected the isolated bufadienolides also in water extracts from both generative and vegetative plant parts, collected in winter as well as in summer (data not shown). Further investigations will be needed to clarify the factors underlying the observed discrepancies.

3. Conclusions

Phytochemical investigation of *H. foetidus* afforded 18 bufadienolides including nine previously undescribed compounds and a congener newly reported as a genuine natural product. These findings considerably extend the knowledge about this group of specialized metabolites in *H. foetidus*. Cytotoxicity assessment on MCF-7 breast cancer cells confirms the role of these compounds in the reported cytotoxic activity of extracts of *H. foetidus* and gives additional insights in the structure-activity relationships. Taken together these data complement the scientific basis underlying the use of this plant for the integrative cancer treatment in anthroposophic medicine. Further experiments are warranted to evaluate the selectivity of the bufadienolides towards cancer cells compared to non-malignant human cells in order to assess their therapeutic potential.

4. Experimental

4.1. Plant material

The aerial parts of *H. foetidus* were collected by one of the authors, D. Shah, in a forest near Bevaix, NE, Switzerland, on January 5, 2022 (GPS coordinates: DD 46.9206, 6.7936 and 46.9278, 6.7923). The taxonomic identification of the plant was carried out by D. Shah. A frozen voucher specimen (no. 1239) is kept at the Division of Pharmaceutical Biology, Department of Pharmaceutical Sciences, University of Basel.

4.2. General experimental procedures

Ultrapure water was obtained from a Milli-Q water purification system (Merck Millipore, Darmstadt, Germany). HPLC-grade acetonitrile, chloroform, dichloromethane, methanol, and formic acid were purchased from Scharlau (Scharlab S.L., Spain). Silica gel 60 F254 coated aluminum TLC plates, and silica gel (0.015–0.040 mm) for open-column chromatography were obtained from Merck KGaA (Darmstadt, Germany). Sephadex LH-20 was obtained from GE Healthcare (Fairfield, CT, USA). Diaion HP-20 was from Supelco (Bellefonte, PA, USA).

HPLC-PDA-CAD-ESIMS analyses were performed on a system consisting of a degasser, a quaternary pump (LC-20AD), a column oven (CTO-20AC), a PDA detector (SPD-M20A), a triple quadrupole mass spectrometer (LCMS-8030) (all Shimadzu, Kyoto, Japan), and a Corona Veo RS Charge aerosol detector (Thermo Scientific, Waltham, MA USA). Separations were performed on a SunFire C₁₈ (3.5 μm, 150 × 3.0 mm i.d.) column equipped with a guard column (10 mm × 3.0 mm i.d.) (Waters, Milford, MA, USA). LabSolutions software (Shimadzu) was used for data acquisition and processing.

Flash chromatography and medium pressure liquid chromatography (MPLC) were performed with a Puriflash 4100 system (Interchim, Montluçon, France) connected to a cartridge or a glass column. Preparative HPLC was carried out on a Preparative LC/MSD System (Agilent Technologies, Santa Clara, CA, USA) consisting of a binary pump (1260 Prep Bin Pump, 1290 Infinity II), a quaternary pump (G1311A Quat Pump, 1200 Series), a 1290 Infinity II Valve Drive manual injection system, a PDA detector (1100 Series), and a Quadrupole LC/MS (6120). A SunFire™ C18 OBD (5 μm, 30 × 150 mm) was used for separation. The flow rate was 20 mL/min. Data acquisition and processing was performed using ChemStation software (Agilent Technologies).

Semi-preparative HPLC separations were performed on an HP 1100

Table 4
Cytotoxic activity of bufadienolides **1–18** against MCF-7 breast cancer cells.

Compound	IC ₅₀ [nM] ^a	95% CI (profile likelihood) ^b
1	1,020	592 to 1,760
2	14.1	11.3 to 17.7
3	1,530	1,090 to 2,170
4	21.4	12.6 to 36.7
5	5.51	3.25 to 9.29
6	6,130	2,950 to 18,400
7	37.7	23.6 to 60.7
8	272	210 to 355
9	1,370	964 to 1,940
10	134	84.4 to 213
11	533	322 to 890
12	6,350	3,620 to 11,600
13	>10,000	–
14	160	92.4 to 284
15	37.6	29.5 to 47.9
16	1.36	0.78 to 2.22
17	35.6	24.2 to 52.1
18	75.9	48.2 to 120
Cisplatin	31,500	19,600 to 44,700

^a Data are reported as mean of three replicates.

^b Curve fitting and CI calculations were performed using Sigmoidal, 4 PL, constraining Hill slope to 1 (Software Prism GraphPad).

Series system (Agilent Technologies) consisting of a binary pump (G1312A BinPump), an autosampler (G1367A WPALS), a column oven (G1316A COLCOM), and a diode array detector (G1315A DAD). A XBridge BEH C18 OBD (5 μ m, 10 \times 150 mm, Waters) was used if not otherwise stated. The flow rate was 4 mL/min. Data acquisition and processing was performed using ChemStation software (Agilent Technologies).

NMR spectroscopic data were recorded on a Bruker Avance III spectrometer (Bruker, Fällanden, Switzerland) operating at 500 MHz for ^1H and 126 MHz for ^{13}C and equipped with a 5 mm BBO probe at 23 $^\circ\text{C}$. Spectra were measured in DMSO- d_6 (ARMAR Chemicals, Döttingen, Switzerland). Chemical shifts are reported in parts per million (δ) using the solvent signal (δ_{H} 2.50; δ_{C} 39.51) as internal reference; coupling constants (J) are given in Hz. Data were analyzed using Topspin (Bruker) and Spectrus Processor (ACD/Labs, Toronto, Canada) softwares. Optical rotation was measured on a JASCO P-2000 polarimeter (Brechtbühler AG, Switzerland) equipped with a 10 cm temperature-controlled microcell. HRESIMS data were recorded on LTQ XL Orbitrap or Q Exactive HF (15) mass spectrometers (both Thermo Scientific, Waltham, MA, USA).

4.3. Extraction and isolation

The fresh plant material (3 kg) was chopped and repeatedly extracted at r.t. with methanol (5.2, 4.0, 4.0, and 4.0 L) over a total of 7 days. The organic solvent was evaporated under reduced pressure and the aqueous residue was suspended in water (1.2 L) and extracted in two portions (650 and 550 mL) with dichloromethane (DCM). The first portion was successively partitioned with 600 mL, 500 mL and 500 mL DCM while 3 \times 550 mL DCM were used for the second portion. The DCM layers were combined and dried under reduced pressure to yield 22.5 g of DCM-soluble fraction. The water layers were further partitioned with *n*-butanol (850 mL, 600 mL, 850 mL and 3 \times 750 mL for the two portions, respectively) to afford, after evaporation to dryness, 40.6 g of *n*-butanol-soluble fraction.

21.6 g of the DCM-soluble fraction were bound on 65 g LiChroprep RP-18 and added to the top of a cartridge already filled with LiChroprep RP-18 (10 \times 4 cm, i.d.). The cartridge was eluted with MeOH 75% to provide, after evaporation to dryness, 11.4 g of a bufadienolide-enriched fraction. This fraction was further separated by MPLC with a gradient of 1–50% MeOH in CHCl_3 . Final purification by semi-preparative HPLC (10–40% MeCN in 30 min) afforded compound **9** (9.5 mg, t_{R} 13.4 min).

A part of the *n*-BuOH-soluble fraction was dissolved in methanol and chromatographed on a Sephadex LH-20 column (88 \times 5 cm, i.d.) in two portions (12 and 15 g, respectively) to afford after TLC analysis 15 fractions (Frs. 1–15). Fraction 7 (16.3 g) was then separated on a column filled with Diaion HP-20 resin (150 g) successively eluted with water and MeOH (both 1.5 L). The MeOH-eluted fraction (2.7 g) was further separated into 13 fractions (Frs. M1–M7) by MPLC on silica gel with a gradient of 10–40% MeOH in CHCl_3 . Separation of Fr. M2 (116 mg) by semi-preparative HPLC with a gradient 10–30% MeCN in 30 min afforded **10** (3.5 mg, t_{R} 10.5 min), **12** (11.7 mg, t_{R} 12.5 min), **16** (2.2 mg, t_{R} 20.0 min), and **17** (9.0 mg, t_{R} 13.5 min). Fraction M3 (138 mg) was separated by semi-preparative HPLC (5–20% MeCN in 30 min) to give **11** (12.9 mg, t_{R} 13.5 min), **18** (16.1 mg, t_{R} 16.0 min), and a fraction which was further purified with 25–30% MeCN to give **8** (3.1 mg, t_{R} 21.0 min). Fraction M6 (349 mg) was separated by preparative HPLC with 20–40% MeCN in 30 min to afford three fractions (Frs. M6.1–M6.3). Further purification of Fr. M6.1 by two successive semi-preparative HPLC steps [XBridge BEH C18 column (see 4.2) with 15% MeCN followed by SunFire C18 column (3.5 mm, 3.0 \times 150 mm, Waters) with 15–25% MeCN in 30 min] gave **1** (2.9 mg). Purification of Fr. M6.2 by semi-preparative HPLC with 15–20% MeCN in 30 min afforded **15** (5.2 mg, t_{R} 20.6 min). Purification of Fr. M6.3 by the same procedure with 20–21% MeCN in 30 min provided **2** (5.5 mg, t_{R} 20.7 min). Fraction M9 (857 mg) was separated by preparative HPLC (5–30% MeCN in 30 min)

to afford five fractions (Frs. M9A–M9E) which were further separated by semi-preparative HPLC. Fraction M9A gave **13** (7.0 mg, t_{R} 13.5 min) with 10% MeCN for 2 min followed by 10–14% B in 30 min; Fr. M9B gave **14** (7.2 mg, t_{R} 21.0 min) with 20–35% MeCN in 30 min; Fr. M9C gave **3** (7.9 mg, t_{R} 16.3 min) and **6** (3.5 mg, t_{R} 18.3 min) with 15% MeCN for 2 min, then 15–20% MeCN in 28 min; Fr. M9D gave **4** (18.0 mg, t_{R} 12.0 min) and **7** (2.8 mg, t_{R} 15.5 min) with 15–19% MeCN in 30 min. Fr. M9E gave **5** (4.2 mg, t_{R} 9.5 min) with 40% MeCN.

4.3.1. Hellefoetin A (5 β ,11 α ,14 β ,19-tetrahydroxy-3 β ,4 β -epoxybufa-20,22-dienolide, **8**)

White amorphous powder; $[\alpha]_{\text{D}}^{24}$ +14.0 (c 0.1, MeOH); UV (MeOH) λ_{max} (log ϵ) 299 nm (3.61); ^1H NMR (500 MHz, DMSO- d_6) and ^{13}C NMR (126 MHz, DMSO- d_6), see Tables 1 and 2; HRESIMS m/z $[\text{M}+\text{H}]^+$ 433.2218 (calcd for $\text{C}_{24}\text{H}_{33}\text{O}_7$ 433.2226).

4.3.2. Hellefoetin B (16 β -formyloxy-5 β ,10 β ,14 β -trihydroxy-3 β ,4 β -epoxy-19-norbufa-20,22-dienolide, **9**)

White amorphous powder; $[\alpha]_{\text{D}}^{24}$ +9.6 (c 0.073, MeOH); UV (MeOH) λ_{max} (log ϵ) 295 nm (3.59); ^1H NMR (500 MHz, DMSO- d_6) and ^{13}C NMR (126 MHz, DMSO- d_6), see Tables 1 and 2; HRESIMS m/z $[\text{M}+\text{H}]^+$ 447.2009 (calcd for $\text{C}_{24}\text{H}_{31}\text{O}_8$ 447.2018).

4.3.3. Hellefoetin C (16 β -formyloxy-5 β ,11 α ,14 β -trihydroxy-3 β ,4 β -epoxy-19-oxobufa-20,22-dienolide, **10**)

White amorphous powder; $[\alpha]_{\text{D}}^{24}$ +19.0 (c 0.042, MeOH); UV (MeOH) λ_{max} (log ϵ) 293 (3.53) nm; ^1H NMR (500 MHz, DMSO- d_6) and ^{13}C NMR (126 MHz, DMSO- d_6), see Tables 1 and 2; HRESIMS m/z $[\text{M}+\text{H}]^+$ 475.1950 (calcd for $\text{C}_{25}\text{H}_{31}\text{O}_9$ 475.1968).

4.3.4. Hellefoetin D (5 β ,11 α ,14 β ,16 β -tetrahydroxy-3 β ,4 β -epoxy-19-oxobufa-20,22-dienolide, **11**)

White amorphous powder; $[\alpha]_{\text{D}}^{24}$ +53.0 (c 0.1, MeOH); UV (MeOH) λ_{max} (log ϵ) 295 nm (3.58); ^1H NMR (500 MHz, DMSO- d_6) and ^{13}C NMR (126 MHz, DMSO- d_6), see Tables 1 and 2; HRESIMS m/z $[\text{M}+\text{H}]^+$ 447.2009 (calcd for $\text{C}_{24}\text{H}_{31}\text{O}_8$ 447.2018).

4.3.5. Hellefoetin E (5 β ,10 β ,14 β ,16 β -tetrahydroxy-3 β ,4 β -epoxy-19-norbufa-20,22-dienolide, **12**)

White amorphous powder; $[\alpha]_{\text{D}}^{24}$ +45.2 (c 0.073, MeOH); UV (MeOH) λ_{max} (log ϵ) 296 nm (3.73); ^1H NMR (500 MHz, DMSO- d_6) and ^{13}C NMR (126 MHz, DMSO- d_6), see Tables 1 and 2; HRESIMS m/z $[\text{M}+\text{H}]^+$ 419.2053 (calcd for $\text{C}_{23}\text{H}_{31}\text{O}_7$ 419.2069).

4.3.6. Hellefoetinoside A (10 β ,14 β ,16 β -trihydroxy-5 β -[(β -D-glucopyranosyl)oxy]-3 β ,4 β -epoxy-19-norbufa-20,22-dienolide, **13**)

White amorphous powder; $[\alpha]_{\text{D}}^{24}$ +35.8 (c 0.067, MeOH); UV (MeOH) λ_{max} (log ϵ) 295 nm (3.75); ^1H NMR (500 MHz, DMSO- d_6) and ^{13}C NMR (126 MHz, DMSO- d_6), see Tables 1 and 3; HRESIMS m/z $[\text{M}+\text{H}]^+$ 581.2591 (calcd for $\text{C}_{29}\text{H}_{41}\text{O}_{12}$ 581.2598).

4.3.7. Hellefoetinoside B (11 α ,14 β -dihydroxy-3 β -[(β -D-glucopyranosyl)oxy]-19-oxobufa-20,22-dienolide, **14**)

White amorphous powder; $[\alpha]_{\text{D}}^{24}$ -17.9 (c 0.067, MeOH); UV (MeOH) λ_{max} (log ϵ) 298 nm (3.69); ^1H NMR (500 MHz, DMSO- d_6) and ^{13}C NMR (126 MHz, DMSO- d_6), see Tables 1 and 3; HRESIMS m/z $[\text{M}+\text{H}]^+$ 579.2814 (calcd for $\text{C}_{30}\text{H}_{43}\text{O}_{11}$ 579.2805).

4.3.8. Hellefoetinoside C (16 β -formyloxy-14 β -hydroxy-5 β -[(β -D-glucopyranosyl)oxy]-19-oxobufa-3,20,22-trienolide, **15**)

White amorphous powder; $[\alpha]_{\text{D}}^{24}$ +79.0 (c 0.1, MeOH); UV (MeOH) λ_{max} (log ϵ) 293 nm (3.77); ^1H NMR (500 MHz, DMSO- d_6) and ^{13}C NMR (126 MHz, DMSO- d_6), see Tables 1 and 3; HRESIMS m/z $[\text{M}+\text{H}]^+$ 605.2602 (calcd for $\text{C}_{31}\text{H}_{41}\text{O}_{12}$ 605.2598).

4.3.9. Hellefoetin F (5 β ,11 α ,14 β -trihydroxy-19-oxobufa-3,20,22-trienolide, **16**)

White amorphous powder; $[\alpha]_D^{24} +50.7$ (c 0.067, MeOH); UV (MeOH) λ_{\max} (log ϵ) 299 nm (3.58); ^1H NMR (500 MHz, DMSO- d_6) and ^{13}C NMR (126 MHz, DMSO- d_6), see [Tables 1 and 3](#); HRESIMS m/z $[\text{M}+\text{H}]^+$ 415.2104 (calcd for $\text{C}_{24}\text{H}_{31}\text{O}_6$ 415.2120).

4.3.10. Hellefoetin G, (16 β -formyloxy-5 β ,11 α ,14 β -trihydroxy-19-oxobufa-3,20,22-trienolide, **17**)

White amorphous powder; $[\alpha]_D^{24} +77.5$ (c 0.08, MeOH); UV (MeOH) λ_{\max} (log ϵ) 295 nm (3.72); ^1H NMR (500 MHz, DMSO- d_6) and ^{13}C NMR (126 MHz, DMSO- d_6), see [Tables 1 and 3](#); HRESIMS m/z $[\text{M}+\text{H}]^+$ 459.2009 (calcd for $\text{C}_{25}\text{H}_{31}\text{O}_8$ 459.2018).

4.3.11. Hellefoetin H (5 β ,11 α ,14 β ,16 β -tetrahydroxy-19-oxobufa-20,22-dienolide, **18**)

White amorphous powder; $[\alpha]_D^{24} +99.0$ (c 0.1, MeOH); UV (MeOH) λ_{\max} (log ϵ) 296 nm (3.70); ^1H NMR (500 MHz, DMSO- d_6) and ^{13}C NMR (126 MHz, DMSO- d_6), see [Tables 1 and 3](#); HRESIMS m/z $[\text{M}+\text{H}]^+$ 431.2074 (calcd for $\text{C}_{24}\text{H}_{31}\text{O}_7$ 431.2069).

4.4. Single crystal X-Ray analysis of compound **8**

Single colourless block-shaped crystals of **8** were obtained in a mixture of EtOH and *n*-hexane. A suitable crystal with dimensions $0.36 \times 0.33 \times 0.30 \text{ mm}^3$ was selected and mounted on a MITIGEN holder in perfluoroether oil on a STOE STADIVARI diffractometer with GaK_α radiation ($\lambda = 1.34143 \text{ \AA}$). The crystal was kept at a steady $T = 150 \text{ K}$ during data collection. The structure was solved with the ShelXT 2018/2 ([Sheldrick, 2015b](#)) solution program using dual methods and by using Olex2 1.5 ([Dolomanov et al., 2009](#)) as the graphical interface. The model was refined with ShelXL 2018/3 ([Sheldrick, 2015a](#)) (using full matrix least squares minimization on F^2). All non-hydrogen atoms were refined anisotropically. Hydrogen atom positions were calculated geometrically and refined using the riding model.

Crystal Data. $\text{C}_{25}\text{H}_{37}\text{O}_8$, $M_r = 475.80$, orthorhombic, $P2_12_12_1$ (No. 19), $a = 7.17870$ (10) \AA , $b = 12.9320$ (2) \AA , $c = 27.4613$ (3) \AA , $\alpha = \beta = \gamma = 90^\circ$, $V = 2549.37$ (6) \AA^3 , $T = 150 \text{ K}$, $Z = 4$, $Z' = 1$, $\mu(\text{GaK}_\alpha) = 0.483$, 38953 reflections measured, 4939 unique ($R_{\text{int}} = 0.0235$) which were used in all calculations. The final wR_2 was 0.1638 (all data) and R_1 was 0.0589 ($I \geq 2 \sigma(I)$). The Hooft parameter was refined to 0.085 (17). The crystallographic data of **8** have been deposited at the Cambridge Crystallographic Data Center (CCDC) (Deposition Number 2386588).

4.5. Single crystal X-ray analysis of compound **11**

Single colourless plate-shaped crystals of **11** were obtained in a mixture of EtOH and *n*-hexane. A suitable crystal with dimensions $0.22 \times 0.16 \times 0.06 \text{ mm}^3$ was selected and mounted on a MITIGEN holder in perfluoroether oil on a STOE STADIVARI diffractometer with CuK_α radiation ($\lambda = 1.54186 \text{ \AA}$). The crystal was kept at a steady $T = 150 \text{ K}$ during data collection. The structure was solved with the ShelXT 2018/2 ([Sheldrick, 2015b](#)) solution program using dual methods and by using Olex2 1.5 ([Dolomanov et al., 2009](#)) as the graphical interface. The model was refined with ShelXL 2018/3 ([Sheldrick, 2015a](#)) using full matrix least squares minimization on F^2 . All non-hydrogen atoms were refined anisotropically. Hydrogen atom positions were calculated geometrically and refined using the riding model.

Crystal Data. $\text{C}_{24}\text{H}_{30}\text{O}_8$, $M_r = 446.48$, orthorhombic, $P2_12_12_1$ (No. 19), $a = 7.2041$ (9) \AA , $b = 11.3490$ (13) \AA , $c = 25.064$ (2) \AA , $\alpha = \beta = \gamma = 90^\circ$, $V = 2049.2$ (4) \AA^3 , $T = 150 \text{ K}$, $Z = 4$, $Z' = 1$, $\mu(\text{Cu K}_\alpha) = 0.900$, 71407 reflections measured, 3947 unique ($R_{\text{int}} = 0.0324$) which were used in all calculations. The final wR_2 was 0.1059 (all data) and R_1 was 0.0388 ($I \geq 2 \sigma(I)$). The Flack parameter was refined to 0.08 (8). The crystallographic data of **11** have been deposited at the Cambridge

Crystallographic Data Center (CCDC) (Deposition Number 2386587).

4.6. Acid hydrolysis and sugar analysis

Experiments were done according to ([Keller et al., 2021](#)) with modifications. Each compound (**13–15**, 0.2–2.0 mg) was hydrolyzed with 2 M HCl (0.5 mL) for 15 h at 100°C . The hydrolysate was extracted with EtOAc ($2 \times 0.5 \text{ mL}$). The aqueous phase was dried under nitrogen and then under high vacuum. The residue was treated with 250 μL of a mixture of (+)-2-butanol and acetyl chloride 10:0.5 (v/v) at 55°C for 15 h. After drying under nitrogen, the residue was derivatized with 250 μL of a mixture of trifluoroacetic anhydride (TFAA) and EtOAc 3:4 (v/v) at 55°C for 1 h. The samples were diluted with 750 μL of HPLC-grade EtOAc and 1 μL was injected using an HTS-PAL 113542 autosampler (CTC-Analytics) into the GCMS (split ratio 1:50). GCMS analysis was performed on a Hewlett-Packard GC-MS system (Agilent G1503A-6890 Plus GC) equipped with a 5973 mass selective detector (MSD) and a 59864B ionization gauge controller (Agilent Technologies). A J&W DB-225 GC column (30 m; 0.25 mm i.d.; film thickness 0.25 μm ; Agilent Technologies) was used. Injector temperature was 280°C . Helium (0.7 mL/min) was used as a carrier gas. Transfer line temperature was 240°C . The following temperature program was applied: 60°C hold for 1 min, increase to 240°C at $10^\circ\text{C}/\text{min}$ followed by 5 min at 240°C . Electron impact (EI) ionization was performed at a temperature of 240°C with an electron energy of 70 eV. Mass scans from m/z 50–700 were recorded. Data acquisition was performed by MSD ChemStation G1701DA D.03.00.611 software (Agilent Technologies) and data were processed with Spectrus Processor (ACD/Labs).

4.7. Cell culture

MCF-7 Breast cancer cells (RRID:CVCL_0031) purchased from ATCC were cultured in DMEM supplemented with 10% FBS in a humidified incubator at 37°C and 5% CO_2 . The medium was changed every 2–3 days and cells were split at a confluency of 80%.

4.8. Cytotoxicity assay

The cytotoxic effects of the substances were determined using a neutral red assay. Briefly, cells were seeded at a density of about 9300 cells per cm^2 . After 24 h of incubation at 37°C , cells were treated with the test substances for 48 h at 37°C . The supernatant was removed and neutral red diluted in cell culture medium (final concentration 25 $\mu\text{g}/\text{L}$) was added to the cells. After 4 h of incubation at 37°C , cells were washed with PBS and desorb solution (49% H_2O , 50% EtOH, 1% CH_3COOH) was added to the cells for 20 min. Optical density was measured in a plate reader at 540 nm. The viability was calculated as a percentage compared to untreated cells. IC_{50} values were determined using GraphPad Prism version 10.1.1 for Windows (GraphPad Software, Boston, Massachusetts USA).

CC-BY authorship contribution statement

Olivier Potterat: Writing – review & editing, Writing – original draft, Supervision, Conceptualization. **Marina Kaufmann**: Investigation. **Cécile Tschopp**: Investigation. **Michaela Caj**: Writing – review & editing, Investigation. **Jakob K. Reinhardt**: Writing – review & editing, Validation, Formal analysis. **Alessandro Prescimone**: Writing – review & editing, Resources, Investigation. **Devika Shah**: Writing – review & editing, Project administration, Funding acquisition, Conceptualization. **Stephan Baumgartner**: Writing – review & editing, Project administration, Funding acquisition, Conceptualization. **Michel-Angelo Sciotti**: Writing – review & editing, Supervision, Project administration, Funding acquisition, Conceptualization. **Laura Suter-Dick**: Writing – review & editing, Supervision, Project administration, Conceptualization.

Declaration of competing interest

The authors declare that they have no known competing financial interests or personal relationships that could have appeared to influence the work reported in this paper.

Acknowledgement

This work was partly supported by an Innosuisse grant (37412.1 IP-LS) to D. Shah, S. Baumgartner and M. Sciotti. Prof. Robin Teufel (Division of Pharmaceutical Biology, University of Basel) is acknowledged for providing the technical infrastructure for the phytochemical investigation. Thanks are due to Dr. Jakob Maier (Hiscia Institute, Arlesheim) for his valuable inputs, to Ms. Nadine Zeis-Kiprijanovski (Division of Pharmaceutical Biology, University of Basel) for her assistance in the isolation of compound **9** and to Dr. Andreas Maximilian Dietl, and Mr. Malik Rakhmanov (both Division of Pharmaceutical Biology, University of Basel) for hydrolysis and sugar analysis of the glucosides and for recording of the HRESIMS data of compound **15**, respectively.

Appendix B. Supplementary data

Supplementary data to this article can be found online at <https://doi.org/10.1016/j.phytochem.2024.114329>.

Data availability

Data will be made available on request.

References

- Djballah, H., Antczak, C., Abramson, D.H., Ambrosi, H.-D., Siems, K., Genski, T., 2013. Compounds for the treatment of ocular cancer. US Patent Application US20130035321A1.
- Dolomanov, O.V., Bourhis, L.J., Gildea, R.J., Howard, J.A.K., Puschmann, H., 2009. Olex2: a complete structure solution, refinement and analysis program. *J. Appl. Crystallogr.* 42, 339–341. <https://doi.org/10.1107/S0021889808042726>.
- Iguchi, T., Uchida, Y., Takano, S., Yokosuka, A., Mimaki, Y., 2020a. Novel steroidal glycosides from the whole plants of *Helleborus foetidus*. *Chem. Pharm. Bull.* 68, 273–287. <https://doi.org/10.1248/cpb.c19-01037>.
- Iguchi, T., Yokosuka, A., Kawahata, R., Andou, M., Mimaki, Y., 2020b. Bufadienolides from the whole plants of *Helleborus foetidus* and their cytotoxicity. *Phytochemistry* 172, 112277. <https://doi.org/10.1016/j.phytochem.2020.112277>.
- Keller, M., Fankhauser, S., Giezendanner, N., König, M., Keresztes, F., Danton, O., Fertig, O., Marcourt, L., Hamburger, M., Butterweck, V., Potterat, O., 2021. Saponins from saffron corms inhibit the gene expression and secretion of pro-inflammatory cytokines. *J. Nat. Prod.* 84, 630–645. <https://doi.org/10.1021/acs.jnatprod.0c01220>.
- Krenn, L., Jelovina, M., Kopp, B., 2000. New bufadienolides from *Urginea maritima* sensu strictu. *Fitoterapia* 71, 126–129. [https://doi.org/10.1016/S0367-326X\(99\)00142-2](https://doi.org/10.1016/S0367-326X(99)00142-2).
- Kubo, I., Matsumoto, T., 1984. Abyssinin, a potent insect antifeedant from an African medicinal plant, *Bersama abyssinica*. *Tetrahedron Lett.* 25, 4601–4604. [https://doi.org/10.1016/S0040-4039\(01\)91210-9](https://doi.org/10.1016/S0040-4039(01)91210-9).
- Kubo, I., Matsumoto, T., 1985. Potent insect antifeedants from the African medicinal plant *Bersama abyssinica*. *ACS Symp. Ser.* 276, 183–200. <https://doi.org/10.1021/bk-1985-0276.ch012>.
- Lichti, H., Niklaus, P., Von Wartburg, A., 1973. Zur Struktur der Scilligliucosids. *Helv. Chim. Acta* 56, 2083–2087. <https://doi.org/10.1002/hlca.19730560633>.
- Meng, Y., Whiting, P., Sik, V., Rees, H.H., Dinan, L., 2001. Ecdysteroids and bufadienolides from *Helleborus torquatus* (Ranunculaceae). *Phytochemistry* 57, 401–407. [https://doi.org/10.1016/S0031-9422\(01\)00070-X](https://doi.org/10.1016/S0031-9422(01)00070-X).
- Meyer, F., Wilkens, J., Rispen, J.A., 2024. *Helleborus foetidus* als aufstrebender Stern in der anthroposophischen Krebstherapie: Darstellung mit Kasuistiken. *Der Merkurstab* 32–37. <https://doi.org/10.14271/DMS-21737-DE>.
- Müller, M.B., Stintzing, F.C., Manukyan, A., Schink, M., 2023. Comparison of cytotoxicity, saponin, and protoanemonin contents of medicinal plant extracts from *Helleborus niger* L. and *Helleborus foetidus* L. *Phytomedicine* 3. <https://doi.org/10.1016/j.phyplu.2023.100424>.
- Potterat, O., Hamburger, M., 2014. Combined use of extract libraries and HPLC-based activity profiling for lead discovery: potential, challenges, and practical considerations. *Planta Med.* 80, 1171–1181. <https://doi.org/10.1055/s-0034-1382900>.
- POWO, 2024. Plants of the World Online. Royal Botanic Gardens, Kew. <https://powo.science.kew.org/>. (Accessed 9 August 2024).
- Prieto, J.M., Siciliano, T., Braca, A., 2006. A new acylated quercetin glycoside and other secondary metabolites from *Helleborus foetidus*. *Fitoterapia* 77, 203–207. <https://doi.org/10.1016/j.fitote.2006.01.012>.
- Sheldrick, G.M., 2015a. Crystal structure refinement with ShelXL. *Acta Crystallogr. C* 71, 3–8. <https://doi.org/10.1107/S2053229614024218>.
- Sheldrick, G.M., 2015b. ShelXT-Integrated space-group and crystal-structure determination. *Acta Crystallogr. E A* 71, 3–8. <https://doi.org/10.1107/S2053273314026370>.
- Tschesche, R., Wirth, W., Welmar, K., 1981. 5-Hydroxyevulinic acid, a new intermediate in the biosynthesis of protoanemonin. *Phytochemistry* 20, 1835–1839. [https://doi.org/10.1016/0031-9422\(81\)84015-0](https://doi.org/10.1016/0031-9422(81)84015-0).
- Watanabe, K., Mimaki, Y., Sakagami, H., Sashida, Y., 2003. Bufadienolide and spirostanol glycosides from the rhizomes of *Helleborus orientalis*. *J. Nat. Prod.* 66, 236–241. <https://doi.org/10.1021/np0203638>.
- WFO, 2024. World Flora Online. <http://www.worldfloraonline.org/>. (Accessed 26 September 2024).
- Yang, F.Y., Su, Y.F., Wang, Y., Chai, X., Han, X., Wu, Z.H., Gao, X.M., 2010. Bufadienolides and phytoecdystones from the rhizomes of *Helleborus thibetanus* (Ranunculaceae). *Biochem. Systemat. Ecol.* 38, 759–763. <https://doi.org/10.1016/j.bse.2010.07.002>.
- Yang, F., Xie, S., Duan, W., Meng, N., Sun, Y., Yu, Y., 2024. Application of bufadienolide compound in preparation of anti-angiogenesis drugs. *Chinese Patent Application CN117357541A*.
- Yokosuka, A., Iguchi, T., Kawahata, R., Mimaki, Y., 2018. Cytotoxic bufadienolides from the whole plants of *Helleborus foetidus*. *Phytochem. Lett.* 23, 94–99. <https://doi.org/10.1016/j.phytol.2017.10.017>.